



## Chronic haloperidol increases voltage-gated Na<sup>+</sup> currents in mouse cortical neurons



Weiqiang Chen<sup>a,b</sup>, Fangfang Zhu<sup>b</sup>, Jingfang Guo<sup>a</sup>, Jiangtao Sheng<sup>b</sup>, Wenli Li<sup>b</sup>, Xiangfeng Zhao<sup>b</sup>, Gefei Wang<sup>b</sup>, Kangsheng Li<sup>b,\*</sup>

<sup>a</sup> Department of Neurosurgery, First Affiliated Hospital, Shantou University Medical College, 57 Changping Road, Shantou, Guangdong 515041, China

<sup>b</sup> Department of Microbiology and Immunology, Key Immunopathology Laboratory of Guangdong Province, Shantou University Medical College, 22 Xinling Road, Shantou, Guangdong 515041, China

### ARTICLE INFO

#### Article history:

Received 9 May 2014

Available online 27 May 2014

#### Keywords:

Haloperidol

Voltage-gated sodium channels

Cortical neurons

Patch-clamp recording

Bromocriptine

BDNF

### ABSTRACT

Typical antipsychotics are characterized by extrapyramidal syndrome (EPS). Previous studies demonstrated that typical antipsychotics could inhibit neuronal voltage-gated sodium channel (VGSC). However, EPS typically emerge only upon prolonged exposure. As a result, we examined effects of haloperidol, a prototype typical antipsychotic, on neuronal VGSC upon incubation for varying duration. Briefly, VGSC currents were activated and recorded using a whole-cell patch-clamp technique in primary culture of mouse cortical neurons. VGSC activity was inhibited by acute haloperidol exposure (for minutes), but enhanced in a time- and concentration-dependent manner by chronic haloperidol exposure (for hours). The effects of chronic haloperidol were associated with increased expression of VGSC subunits as well as corresponding electrophysiological channel properties. In summary, we found enhanced VGSC currents upon chronic haloperidol exposure in cortical neurons in contrast to inhibition by acute haloperidol exposure. Such a results may contribute to EPS of typical antipsychotics.

© 2014 The Authors. Published by Elsevier Inc. This is an open access article under the CC BY-NC-ND license (<http://creativecommons.org/licenses/by-nc-nd/3.0/>).

## 1. Introduction

Typical antipsychotics exemplified by haloperidol form the basis of psychosis treatment [1], and are occasionally used to manage Tourette's syndrome [2], nausea, and vomiting [3]. These agents have high affinity for D<sub>2</sub> dopamine receptors [4]. A major limitation of typical antipsychotics is extrapyramidal syndrome (EPS) [5,6].

The pharmacological actions of haloperidol, including the EPS, were previously thought to be mainly mediated by blockade of dopamine receptors [7,8]. However, recent research also implicated multiple ion channels. For example, typical antipsychotics (e.g., haloperidol and pimozide) could block L-type [9] and T-type calcium channels [10]. Inhibition of calcium-activated potassium channels has also been found for phenothiazine-derivatives [11,12]. Off-target effects at the hERG potassium channel have linked to cardiac liability of several antipsychotics [13].

Voltage-gated Na<sup>+</sup> channels (VGSCs) consist of pore-forming  $\alpha$ -subunits (220–260 kDa) and auxiliary  $\beta$ -subunits (32–36 kDa) [14]. VGSCs regulate the regeneration and propagation of action

potentials (AP) by mediating the inward Na<sup>+</sup> current in excitable cells [15,16]. Knockout of fibroblast growth factor homologous factors in mice inhibits the APs via modifying electrophysiological properties of VGSCs [17]. VGSCs also affect the resting potential of neurons, and the threshold for AP generation [18].

Previous studies demonstrated that acute haloperidol treatment could inhibit neuronal VGSCs [19]. In the present study, we examined the effects of haloperidol (0.1–25  $\mu$ M) on VGSC in cultured mouse cortical neurons upon varying exposure time (4–48 h) with patch-clamp. Effects on VGSC subunits were examined at the protein levels.

## 2. Materials and methods

### 2.1. Cortical neuron culture

The primary culture of mouse cortical neurons was established using 14-day-old (E14) C57 BL/6J mouse embryos, as previously reported [20]. Briefly, cerebral cortices (containing no hippocampus) were trypsinized for 2 min with 4-ml 0.25% trypsin (Invitrogen) at 37 °C and then interrupted with 0.5-ml fetal bovine serum (HyClone). Cells were collected by centrifugation for 10 min at 900 $\times$ g, re-suspended in minimum essential medium

\* Corresponding author.

E-mail address: [kсли@stu.edu.cn](mailto:kсли@stu.edu.cn) (K. Li).

(Invitrogen), and seeded in 22 mm × 22 mm glass cover slip pre-treated with 12.5 µg/ml poly-D-lysine (Sigma) at  $1 \times 10^6$  per well. Glutamine (Sigma; 2 mM) and 2% B-27 supplement were added into the neurobasal medium immediately before use. Cells were incubated in 2-ml culture medium in 35-mm petri dishes at 37 °C in 5% CO<sub>2</sub>/95% air. Half of the culture medium was changed every 3 days. A selective inhibitor of DNA synthesis, arabinosylcytosine C (4 µM), was added to the medium on day 3 for 24 h to eliminate glial cells. All experiments were performed after 8–12 days. The animals used in this study were housed and treated according to the guidelines for care and use of experimental animals of the Ethics Committee of Shantou University Medical College.

## 2.2. Electrophysiological recording

Electrophysiological recording was carried out as previously reported [20]. The bath solution composed of 140 mM NaCl, 5 mM KCl, 1 mM MgCl<sub>2</sub>, 2 mM CaCl<sub>2</sub>, 10 mM HEPES, 4 mM TEA-Cl, 0.1 mM CdCl<sub>2</sub> and 10 mM glucose (pH adjusted to 7.3 with NaOH) for whole-cell recording of voltage-gated Na<sup>+</sup> currents. The pipette solution contained 145 mM CsCl, 1 mM MgCl<sub>2</sub>, 1 mM CaCl<sub>2</sub>, 1 mM EGTA, 10 mM HEPES, and 5 mM ATP-Na<sub>2</sub> (pH adjusted to 7.3 with CsOH). Patch pipettes were pulled to a tip resistance of 2–5 MΩ from a borosilicate glass capillary using a P-97 micropipette puller (Sutter Instrument). Voltage-clamp recording was performed using an EPC-10 amplifier (HEKA). Series resistance was compensated by 70–90%. Data were digitized at 200 kHz. Neurons were held at –80 mV and then depolarized to 100 mV with 5-mV steps (each 20 ms) and 0.5 Hz frequency to examine the activation of VGSCs. Na<sup>+</sup> currents were recorded at 0 mV after prepulse from –100 mV to 30 mV for 40 ms with 5-mV steps to examine the inactivation of VGSCs.

APs were recorded in a current clamp mode to measure the threshold and firing rate of the spike. Cells were held at 0 pA, and APs were elicited by depolarizing currents ranging from –50 pA to 70 pA (120 ms) with increments of 10 pA or a ramp current of 0–500 pA (100 ms). The external solution contained 140 mM NaCl, 3 mM KCl, 2 mM MgCl<sub>2</sub>, 0.1 mM CdCl<sub>2</sub>, 1 mM CaCl<sub>2</sub>, and 10 mM HEPES (pH adjusted to 7.3 with NaOH). The pipette solution contained 140 mM KCl, 10 mM EGTA, 5 mM Mg-ATP, and 5 mM HEPES (pH adjusted to 7.3 with KOH). All experiments were performed at 23–25 °C.

## 2.3. Drug application

In acute experiments, cells were exposed to haloperidol at 0.1–250 µM in extracellular solution for 5 min. In chronic experiments, cells were exposed to haloperidol (25–100 µM) for 2–48 h. The D2 receptor agonist bromocriptine (10 µM) was present in some experiments for 1 h before and during haloperidol (25 µM 24 h) treatment. Brain derived neurotrophic factor (BDNF; 30 ng/ml) was present in some experiment with haloperidol (25 µM 24 h).

## 2.4. Immunoblot

Membrane fraction was prepared using discontinuous sucrose gradient centrifugation. Briefly, whole-brain lysate in 0.32 M sucrose/5 mM Tris (pH 7.4) were layered onto 1.2 M sucrose/5 mM Tris (pH 7.4), and centrifuged at 10,000×g for 30 min. The 0.8 M to 1.2 M sucrose interface was collected, diluted twofold with 0.8 M sucrose/5 mM Tris (pH 7.4), and centrifuged at 20,000×g for 20 min. The resulting pellet was re-suspended in RIPA buffer containing 25 mM Tris, 150 mM NaCl, 1 mM EDTA, and 2% Triton X-100 (pH 7.4), and centrifuged at 20,000×g for 20 min to yield the final membrane preparation (supernatant). Complete protease

inhibitor (Roche) was included during the entire procedure. Membrane preparation (100-mg protein) was fractionated by SDS-PAGE, and transferred onto a nitrocellulose membrane (Millipore). The membrane was blocked in 5% nonfat milk and then incubated with a mouse anti-pan Nav antibody (1:200; Alomone) overnight at 4 °C, followed by incubation with a horseradish peroxidase-conjugated secondary antibody (anti-mouse 1:1,000; Sigma) and visualization through chemiluminescence.

## 2.5. Statistical analysis

Data are expressed as mean ± SEM, and analyzed using Origin software (Origin Lab Corporation, Northampton, USA) and SPSS 15.0 (SPSS Inc., USA). The normative Na<sup>+</sup> current amplitudes, current density (pA/pF), current concentration dependency, time dependency, and protein expression level were evaluated and compared using one-way ANOVA followed by SNK test. The activation and inactivation of VGSCs, thresholds, and the firing rate of spikes were analyzed with Student's *t*-test.

## 3. Results

The Na<sup>+</sup> currents were completely blocked with TTX (300 µM) (Fig. 1A).

### 3.1. Effects of haloperidol on Na<sup>+</sup> currents

#### 3.1.1. Acute vs. chronic exposure

Acute exposure to haloperidol (for 5 min) decreased the Na<sup>+</sup> currents by 22% ± 2.27%, 52% ± 2.52%, and 85.82% ± 0.85% at 10, 25, and 250 µM (Fig. 1B and C; IC<sub>50</sub> = 19.38 M). The inhibitory effect of haloperidol was reversible upon washout (Fig. 1B).

An inward current with fast activation and inactivation was elicited by depolarization steps from –80 mV of the holding potential and recorded at 200 kHz of the sampling frequency (Fig. 1D). Haloperidol treatment for 24 h significantly enhanced the voltage-gated Na<sup>+</sup> currents at most activated potentials (Fig. 1E and F). The increase of Na<sup>+</sup> currents was 57% ± 4.48%, 143% ± 5.42% and 145% ± 4.27% at 10, 25 and 100 µM, respectively. The peak currents at –20 mV plotted against haloperidol concentration indicated that the enhancement was concentration-dependent (Fig. 1F).

### 3.2. Time-dependent effects of haloperidol on Na<sup>+</sup> currents

Upon haloperidol treatment (25 µM) for 30 min, the Na<sup>+</sup> currents were increased after 24–48 h, but not 1–8 h (Fig. 1G). Haloperidol treatment (100 µM) for 30 min increased Na<sup>+</sup> currents after 8–24 h but not earlier; neuronal death was noted after 48 h.

### 3.4. Effects of haloperidol on Na<sup>+</sup> channel kinetics

Fig. 2 is representative conductance-voltage curve, fitted using the Boltzmann equation (Fig. 2A). Channel inactivation was reflected using the peak currents at 0 mV of the test voltage, normalized using the maximal current (Fig. 2B). Normative currents were plotted to the pre-pulse voltage, while the current-voltage curves were fitted using the Boltzmann equation (Fig. 2B).

Acute perfusion with haloperidol (25 µM) accelerated the inactivation of Na<sup>+</sup> channels (Fig. 2A), but did not affect activation properties (Fig. 2B). In contrast, chronic haloperidol treatment accelerated the activation of Na<sup>+</sup> channels, but did not affect inactivation properties (Fig. 2C and D).

Immunoblot assay of VGSCs using a pan-antibody in the cell membrane (Fig. 3A and B) showed that 24-h haloperidol treatment

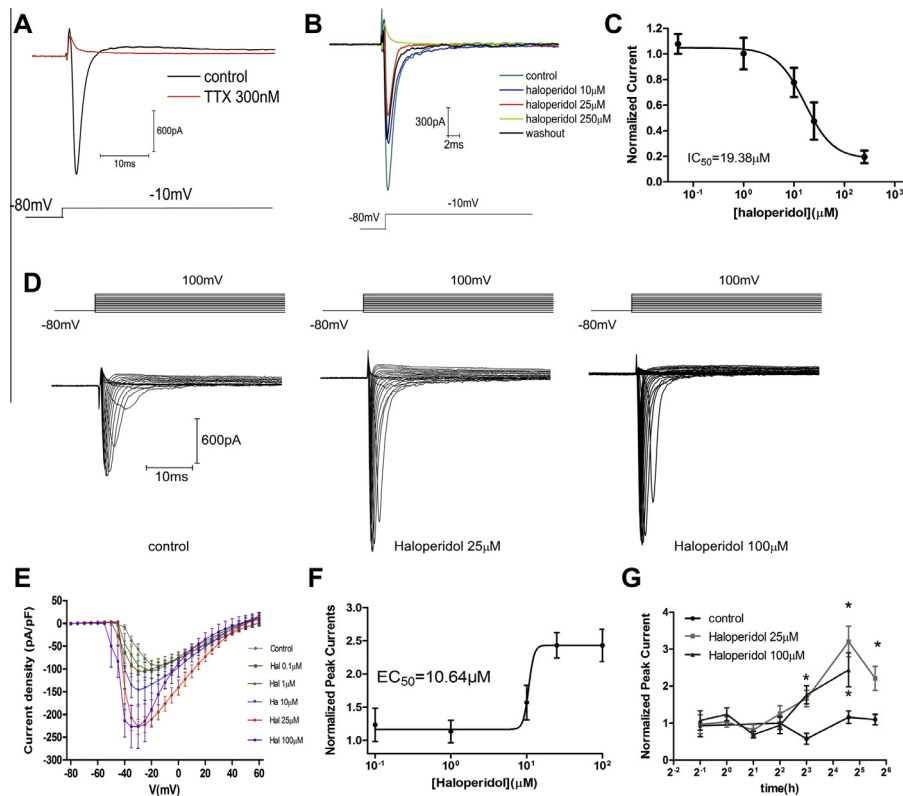


**Fig. 1.** Effects of haloperidol on  $\text{Na}^+$  currents. (A) Representative recording of whole-cell currents in the presence or absence of TTX (300  $\mu\text{M}$ ). (B) Representative recording of whole-cell  $\text{Na}^+$  currents upon acute perfusion with haloperidol (10, 25 or 250  $\mu\text{M}$ ). (C) The concentration–response relationship for haloperidol inhibition of the  $\text{Na}^+$  currents;  $\text{IC}_{50} = 19.38 \mu\text{M}$ . (D) Recording of whole-cell  $\text{Na}^+$  currents from  $-80$  to  $100$  mV upon 24-h exposure to haloperidol (25 and 100  $\mu\text{M}$ ). (E) Current–density–voltage relationship upon 24-h exposure to haloperidol (0.1–100  $\mu\text{M}$ ). (F) Concentration-dependent effects of 24-h haloperidol treatment (0.1–100  $\mu\text{M}$ ) on  $\text{Na}^+$  currents;  $\text{EC}_{50} = 10.64 \mu\text{M}$ . (G) Time-dependent effects of haloperidol (25 and 100  $\mu\text{M}$ ) on  $\text{Na}^+$  currents. Current data were normalized by control and expressed as percentage of the control. \* $P < 0.05$  compared with the control (one-way ANOVA followed by SNK).

(25  $\mu\text{M}$ ) increased the number of VGSCs in the cell membrane by  $56\% \pm 3.7\%$  ( $P < 0.05$ ).

### 3.3. Effects of bromocriptine and BDNF

Pretreatment with bromocriptine (10  $\mu\text{M}$ ) or BDNF (30 ng/ml), starting from 30 min prior to haloperidol treatment blocked the haloperidol effects on  $\text{Na}^+$  currents (Fig. 3C and D). However, neither the activation nor inactivation of the  $\text{Na}^+$  channels was significantly affected by bromocriptine or BDNF (Fig. 3E and F).

### 3.4. Effects of haloperidol on the amplitude and threshold of the spike

Acute perfusion with haloperidol (25  $\mu\text{M}$ ) abolished the AP in cortical neurons (Fig. 4A–D). Haloperidol treatment (25  $\mu\text{M}$ ) for 24-h decreased the threshold of the spike (Fig. 4E–G), and increased the firing rate (Fig. 4H–J).

## 4. Discussion

Major findings of the current study include: (1) acute haloperidol exposure inhibits VGSC activity by accelerating the inactivation of  $\text{Na}^+$  channels in a concentration-dependent manner; (2) chronic haloperidol exposure enhances voltage-gated  $\text{Na}^+$  currents in a time- and concentration-dependent manner by accelerating the activation of  $\text{Na}^+$  channels. Another finding is chronic haloperidol potentiation on VGSCs can be counteracted by bromocriptine and BDNF.

### 4.1. Mechanism of the effects of haloperidol on $\text{Na}^+$ currents

Acute haloperidol shifted the steady-state inactivation curve to the left. Channel activation was not affected. The inhibitory effect of haloperidol is largely reversible upon washout. Perhaps more time was needed for complete recovery of the peak amplitude of  $\text{Na}^+$  currents.

Effects of chronic haloperidol treatment on cortical neurons are mediated by D2 receptor inhibition [21]. The D2 receptor agonist bromocriptine blocked haloperidol-induced increases of  $\text{Na}^+$  currents. Previous studies demonstrated that bromocriptine could successfully treat Neuroleptic malignant syndrome [22,23], and protect neurons against 6-hydroxydopamine damage via its hydroxyl free radical scavenging activity and inhibition of dopamine turnover [24]. Alternatively, bromocriptine's effects might be attributable to GPCR-mediated modulation of channel function. Indeed, dopamine receptor activation has been shown to influence both sodium and calcium channel function indirectly, possibly by modulating channel phosphorylation [25]. Regulation of sodium channel activity has been reported in certain neuronal populations following D2 receptor stimulation [26]. All together, our results suggest that VGSC alterations in neurons likely contribute to haloperidol-induced EPS, which could be relieved by bromocriptine-induced VGSCs inhibition.

Previous study had highlighted the therapeutic potential of BDNF in a range of CNS disorders – including Alzheimer's disease, stroke and depression [27]. The results from the current study showed that BDNF could block haloperidol-induced increases of  $\text{Na}^+$  currents, raising the possibility that BDNF could protect against haloperidol-induced EPS.

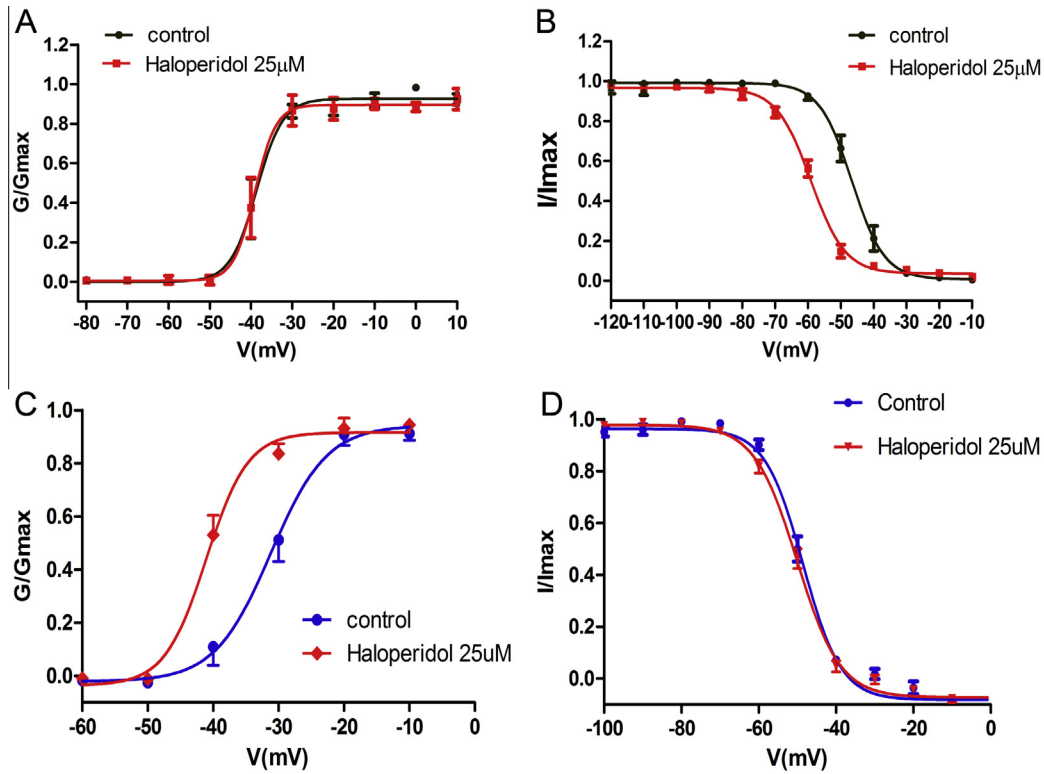


**Fig. 2.** Effects of haloperidol on Na<sup>+</sup> channel kinetics. (A) Voltage-dependent activation upon acute perfusion with haloperidol (25 μM) vs. blank control groups. (B) Voltage-dependent fast-inactivation upon acute perfusion with haloperidol (25 μM) vs. blank control. (C) Voltage-dependent activation upon 24-h haloperidol treatment (25 μM) vs. the control. (D) Representative inactivation properties, and voltage-dependent inactivation upon 24-h haloperidol treatment (25 μM) vs. the control.

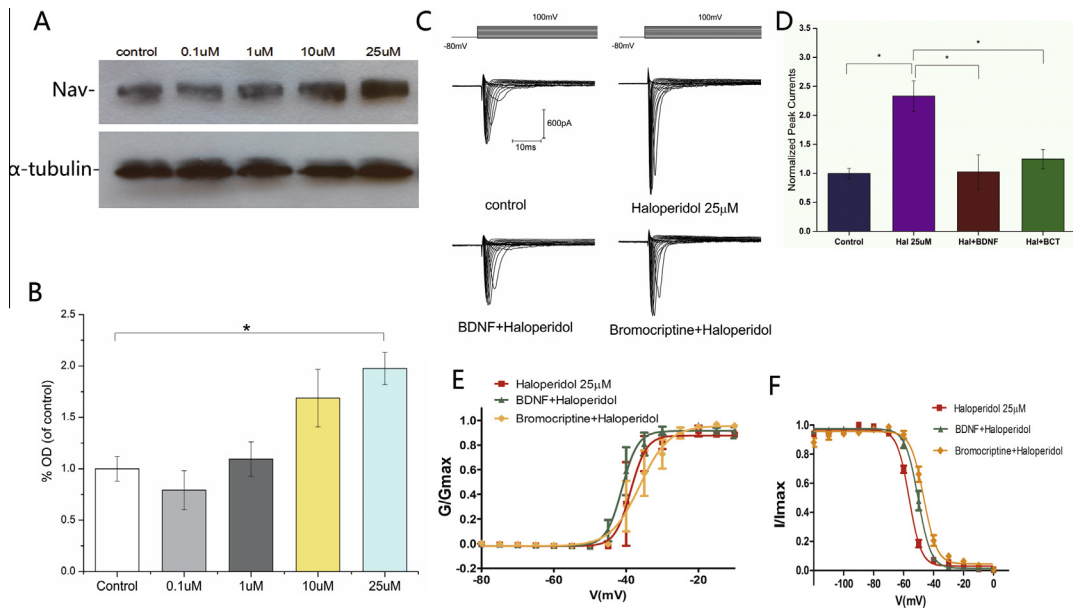


**Fig. 3.** Effects of haloperidol on VGSCs expression and effects of bromocriptine and BDNF on haloperidol's augmentation of Na<sup>+</sup> currents. (A) Representative immunoblot of Nav channels protein in the cell membrane upon 24-h haloperidol exposure (25 μM) group vs. blank control. (B) Summary of haloperidol effects on VGSCs expression. Values represent three separate experiments performed in duplicate. (C) An illustration of the recording curves of whole-cell Na<sup>+</sup> currents from -80 mV to 100 mV in the control and haloperidol (25 μM, 24 h), haloperidol + bromocriptine, and haloperidol + BDNF groups. (D) Normalized peak currents in the control and haloperidol (25 μM, 24 h), haloperidol + bromocriptine, and haloperidol + BDNF groups. (E) Voltage-dependent activation curves in the control and haloperidol (25 μM, 24 h), haloperidol + bromocriptine, and haloperidol + BDNF groups. (F) Voltage-dependent inactivation curves in the control and haloperidol (25 μM, 24 h), haloperidol + bromocriptine, and haloperidol + BDNF groups. \**P* < 0.05 compared with the control and/or haloperidol (25 μM, 24 h) group (one-way ANOVA followed by SNK).

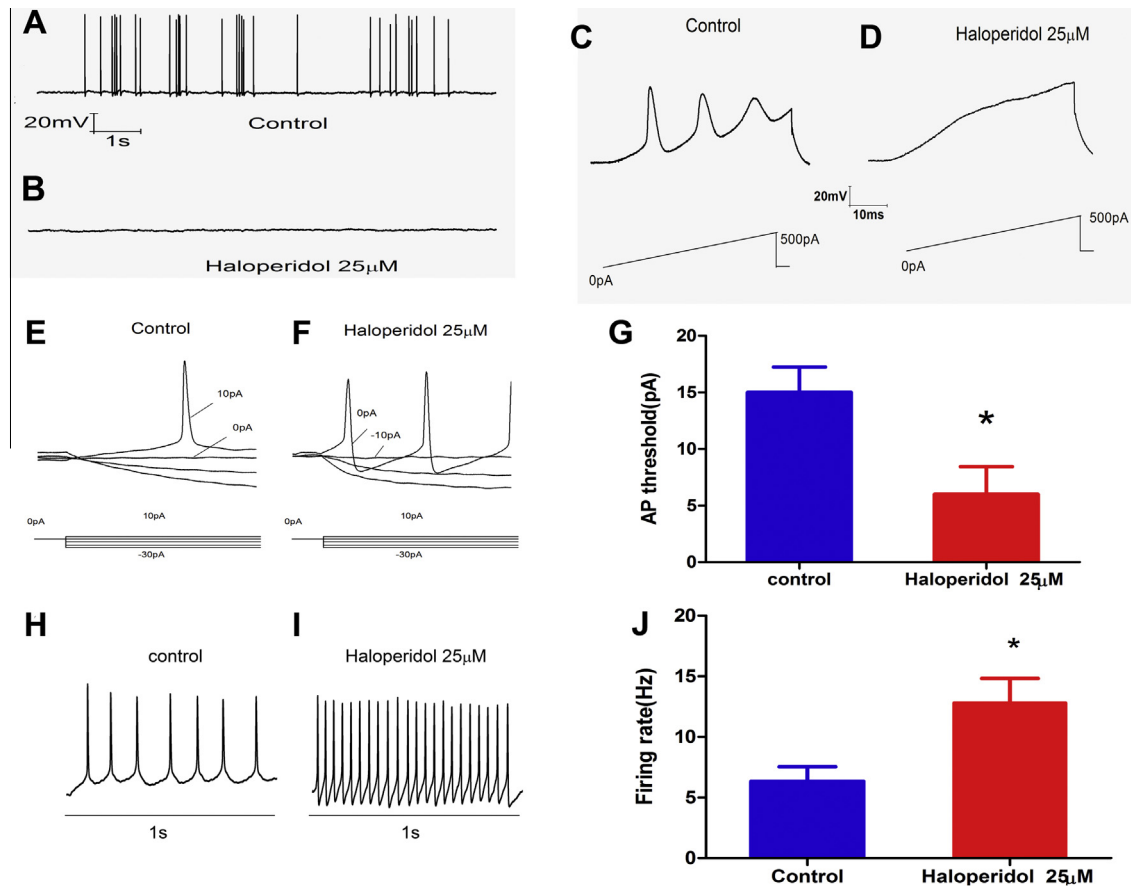


**Fig. 4.** Effects of haloperidol on action potentials. (A) Representative recording showing traces of action potentials. (B) Haloperidol perfusion (25  $\mu$ M) abolished the action potential. (C and D) Representative spike elicited by a ramp depolarizing current in the blank control (C) vs. haloperidol (25  $\mu$ M) (D). (E and F) Representative recordings of action potentials, and decrease of AP threshold by 24-h haloperidol treatment (25  $\mu$ M). (G) Summary of haloperidol effects (25  $\mu$ M for 24 h) on AP threshold ( $*P < 0.05$ ,  $n = 10$ /group). (H and I) Representative recordings of firing rate of AP in response to current injection (500 pA, 1 s) in the control neuron vs. upon haloperidol treatment (25  $\mu$ M for 24 h). (J) Summary of haloperidol effects (25  $\mu$ M for 24 h) on the firing rate ( $*P < 0.05$ ,  $n = 8$ /group). Statistical analysis was carried out with Student's *t*-test.

#### 4.2. Potential neurotoxicity of chronic haloperidol due to increased $\text{Na}^+$ currents

The selection of haloperidol concentration (0.1–25  $\mu$ M) for the current study was based on concentrations reported in the brain tissue of patients, especially tardive dyskinesia (TD) patients, during long-term therapeutic treatment with haloperidol [21,28].

Augmentation of  $\text{Na}^+$  currents in injured neurons increases the consumption of energy used to maintain the  $\text{Na}^+$  gradient across the plasma membrane [29]. Therefore, haloperidol amplification of  $\text{Na}^+$  currents in cortical neurons may reduce neuronal survival in injuries and diseases of the CNS. An exemplification of this is a spike that was recorded using the current-clamp technique in our experimental conditions, which showed that the AP amplitude was significantly higher in the haloperidol (25  $\mu$ M, 24 h) treatment group after using a ramp pulse current (0–500 pA) to measure AP. This result is consistent with the current density recording results showing that haloperidol increases neuronal excitability. Previously studies showed that haloperidol could promote neuronal death by increasing  $\text{Ca}^{2+}$  entry into the neurons [30–32]. An increase in AP amplitude and firing rate may enhance  $\text{Ca}^{2+}$  influx through voltage-gated  $\text{Ca}^{2+}$  channels during the spike, and exacerbate the damage of injured neurons induced by  $\text{Ca}^{2+}$  overload. Excitotoxicity resulting from the excessive release of excitatory transmitters from the presynaptic membrane, putatively caused by increased AP amplitude and firing rate, is involved in many brain diseases and injuries [32,33]. Based on the findings of increased AP firing rate and amplitude,

we speculate that haloperidol could promote the release of neurotransmitters from the presynaptic terminal and exhibit neurotoxic effects on the CNS.

In summary, our results suggest that haloperidol enhances the activity of VGSCs in cortical neurons upon prolonged exposure in contrast to previous reports of channel inhibition upon acute haloperidol exposure, and both bromocriptine and BDNF counteract the VGSC potentiation induced by haloperidol. We speculate that such time-dependent effects contribute to the time dependency of both therapeutic effects and side effects of haloperidol. In addition, the findings prompt the therapeutic potential of BDNF on haloperidol-induced EPS.

#### Acknowledgments

We are grateful to Dr. Yingji Li from ICE Bioscience Inc. for assistance on electrophysiological experiments. This project was supported by the National Natural Science Foundation of China (31170852, 81001322 and 81172795).

#### References

- [1] J. Geddes, N. Freemantle, P. Harrison, P. Bebbington, Atypical antipsychotics in the treatment of schizophrenia: systematic overview and meta-regression analysis, *BMJ* 321 (2000) 1371–1376.
- [2] M.J. Schwabe, R.J. Konkol, Treating Tourette syndrome with haloperidol: predictors of success, *Wis. Med. J.* 88 (1989) 23–27.
- [3] J.R. Hardy, A. O'Shea, C. White, K. Gilshenan, L. Welch, C. Douglas, The efficacy of haloperidol in the management of nausea and vomiting in patients with cancer, *J. Pain Symptom Manage.* 40 (2010) 111–116.

- [4] L. Brand, D.W. Oliver, C.J. van der Schyf, S.M. Pond, N. Castagnoli Jr., Dopamine receptor binding of 4-(4-chlorophenyl)-1-[4-(4-fluorophenyl)-4-oxobutyl]-1,2,3,6-tetrahydropyridine (HPTP), an intermediate metabolite of haloperidol, *Life Sci.* 59 (1996) 815–820.
- [5] B.J. Robottom, L.M. Shulman, W.J. Weiner, Drug-induced movement disorders: emergencies and management, *Neurol. Clin.* 30 (2012) 309–320.
- [6] J.M. Kane, J.M. Davis, N. Schooler, S. Marder, D. Casey, B. Brauzer, J. Mintz, R. Conley, A multidose study of haloperidol decanoate in the maintenance treatment of schizophrenia, *Am. J. Psychiatry* 159 (2002) 554–560.
- [7] A. Bartolomeis, E.F. Buonaguro, F. Iasevoli, Serotonin–glutamate and serotonin–dopamine reciprocal interactions as putative molecular targets for novel antipsychotic treatments: from receptor heterodimers to postsynaptic scaffolding and effector proteins, *Psychopharmacology* 225 (2013) 1–19.
- [8] T. Sakurai, A. Amemiya, M. Ishii, I. Matsuzaki, R.M. Chemelli, H. Tanaka, S.C. Williams, et al., Orexins and orexin receptors: a family of hypothalamic neuropeptides and G protein-coupled receptors that regulate feeding behavior, *Cell* 92 (1998) 573–585.
- [9] K. Ito, K. Nakazawa, S. Koizumi, M. Liu, K. Takeuchi, T. Hashimoto, Y. Ohno, K. Inoue, Inhibition by antipsychotic drugs of L-type  $Ca^{2+}$  channel current in PC12 cells, *Eur. J. Pharmacol.* 314 (1996) 143–150.
- [10] C.M. Santi, F.S. Cayabyab, K.G. Sutton, J.E. McRory, J. Mezeyova, K.S. Hamming, D. Parker, et al., Differential inhibition of T-type calcium channels by neuroleptics, *J. Neurosci.* 22 (2002) 396–403.
- [11] K. Lee, F. McKenna, I.C. Rowe, M.L. Ashford, The effects of neuroleptic and tricyclic compounds on BKCa channel activity in rat isolated cortical neurons, *Br. J. Pharmacol.* 121 (1997) 1810–1816.
- [12] G.C. Terstappen, G. Pula, C. Carignani, M.X. Chen, R. Roncarati, Pharmacological characterization of the human small conductance calcium-activated potassium channel hSK3 reveals sensitivity to tricyclic antidepressants and antipsychotic phenothiazines, *Neuropharmacology* 40 (2001) 772–783.
- [13] S. Kongsamut, J. Kang, X.L. Chen, J. Roehr, D. Rampe, A comparison of the receptor binding and HERG channel affinities for a series of antipsychotic drugs, *Eur. J. Pharmacol.* 450 (2002) 37–41.
- [14] W.A. Catterall, From ionic currents to molecular mechanisms: the structure and function of voltage-gated sodium channels, *Neuron* 26 (2000) 13–25.
- [15] A.L. Hodgkin, A.F. Huxley, A quantitative description of membrane current and its application to induction and excitation in nerve, *J. Physiol.* 117 (1952) 500–544.
- [16] B. Hille, *Ion Channels of Excitable Membranes*, Sinauer Associates Inc., Sunderland, MA, 2001.
- [17] M. Goldfarb, J. Schoorlemmer, A. Williams, S. Diwakar, Q. Wang, X. Huang, J. Giza, et al., Fibroblast growth factor homologous factors control neuronal excitability through modulation of voltage-gated sodium channels, *Neuron* 55 (2007) 449–463.
- [18] A.M. Rush, T.R. Cummins, Painful research: identification of a small-molecule inhibitor that selectively targets Nav1.8 sodium channels, *Mol. Interv.* 7 (2007) 192–195.
- [19] M. Wakamori, M. Kaneda, Y. Oyama, N. Akaike, Effects of chlordiazepoxide, chlorpromazine, diazepam, diphenylhydantoin, flunitrazepam and haloperidol on the voltage-dependent sodium current of isolated mammalian brain neurons, *Brain Res.* 494 (1989) 374–378.
- [20] C. Zhou, C. Qi, J. Zhao, F. Wang, W. Zhang, C. Li, et al., Interleukin-1 $\beta$  inhibits voltage-gated sodium currents in a time- and dose-dependent manner in cortical neurons, *Neurochem. Res.* 36 (2011) 1116–1123.
- [21] W. Ukai, H. Ozawa, M. Tateno, E. Hashimoto, T. Saito, Neurotoxic potential of haloperidol in comparison with risperidone: implication of Akt-mediated signal changes by haloperidol, *J. Neural. Transm.* 111 (2004) 667–681.
- [22] P.S. Mueller, J.W. Vester, J. Fermaglich, Neuroleptic malignant syndrome: successful treatment with bromocriptine, *JAMA* 249 (1983) 386–388.
- [23] J.E. Granato, B.J. Stern, A. Ringel, et al., Neuroleptic malignant syndrome: successful treatment with dantrolene and bromocriptine, *Ann. Neurol.* 14 (1983) 89–90.
- [24] N. Ogawa, K. Tanaka, M. Asanuma, M. Kawai, T. Masumizu, M. Kohno, A. Mori, Bromocriptine protects mice against 6 hydroxydopamine and scavenges hydroxyl free radical in vitro, *Brain Res.* 657 (1994) 207–213.
- [25] A.R. Cantrell, T. Scheuer, W.A. Catterall, Voltage-dependent neuromodulation of  $Na^{+}$  channels by D1-like dopamine receptors in rat hippocampal neurons, *J. Neurosci.* 19 (1999) 5301–5310.
- [26] N. Maurice, J. Mercer, C.S. Chan, S. Hernandez-Lopez, J. Held, T. Tkatch, D.J. Surmeier, D2 dopamine receptor-mediated modulation of voltage-dependent  $Na^{+}$  channels reduces autonomous activity in striatal cholinergic interneurons, *J. Neurosci.* 4 (2004) 10289–10301.
- [27] A.H. Nagahara, M.H. Tuszynski, Potential therapeutic uses of BDNF in neurological and psychiatric disorders, *Nat. Rev. Drug Discovery* 10 (2011) 209–219.
- [28] J. Kornhuber, A. Schultz, J. Wiltfang, I. Meineke, C.H. Gleiter, R. Zöchling, K.W. Boissl, et al., Persistence of haloperidol in human brain tissue, *Am. J. Psychiatry* 156 (1999) 885–890.
- [29] X.Q. Wang, A.Y. Xiao, C. Sheline, K. Hycr, A. Yang, M.P. Goldberg, et al., Apoptotic insults impair  $Na^{+}$ ,  $K^{+}$ -ATPase activity as a mechanism of neuronal death mediated by concurrent ATP deficiency and oxidant stress, *J. Cell Sci.* 166 (2003) 2099–2110.
- [30] A. Lillienbaum, A. Israël, From calcium to NF-kappa signaling pathways in neurons, *Mol. Cell. Biol.* 23 (2003) 2680–2698.
- [31] H.Z. Yin, C.I. Hsu, S. Yu, S.D. Rao, L.S. Sorkin, J.H. Weiss, TNF- $\alpha$  triggers rapid membrane insertion of  $Ca^{2+}$  permeable AMPA receptors into adult motor neurons and enhances their susceptibility to slow excitotoxic injury, *Exp. Neurol.* 238 (2012) 93–102.
- [32] D. Jabaudon, M. Scanziani, B.H. Gähwiler, U. Gerber, Acute decrease in net glutamate uptake during energy deprivation, *Proc. Natl. Acad. Sci. U.S.A.* 97 (2000) 5610–5615.
- [33] Y. Nishizawa, Glutamate release and neuronal damage in ischemia, *Life Sci.* 69 (2001) 369–381.